American Mineralogist, Volume 80, pages 9–20, 1995

A transitional structural state and anomalous Fe-Mg order-disorder in Mg-rich orthopyroxene, $(Mg_{0.75}Fe_{0.25})_2Si_2O_6$

HEXIONG YANG, SUBRATA GHOSE
Mineral Physics Group, Department of Geological Sciences, University of Washington, Seattle, Washington 98195, U.S.A.

ABSTRACT

From in-situ structure and site occupancy refinements of a synthetic orthopyroxene, $(Mg_{0.75}Fe_{0.25})_2Si_2O_6$, by single-crystal X-ray diffraction at 296, 1000, 1100, 1200, and 1300 K (with reversals), two significant phenomena were observed: (1) with increasing temperature, the silicate B chain straightens much faster, especially above 1200 K, and becomes straighter than the A chain at 1300 K, with the O3-O3-O3 angles of the A and B chains being 170.8 and 173.1°, respectively; and (2) the ln K_D values (where $K_D = Fe^{M1}Mg^{M2}/Fe^{M2}Mg^{M1}$) vary linearly with $1/T$ (K) between 1000 and 1200 K, but nonlinearly between 1200 and 1300 K. The drastic straightening of the silicate chains at 1300 K is accompanied by the attainment of very similar configurations of the SiO_4 tetrahedra, SiA and SiB, in shapes, sizes, and out-of-plane tiltings. The rigid-body thermal vibration analysis suggests that the librational motion of the SiA tetrahedron (8.1°²) is slightly larger than that of SiB (5.2°²) at 296 K but becomes considerably smaller (48.0°²) than that of SiB (77.3°²) at 1300 K. The M1 octahedron remains nearly regular from 296 to 1300 K, whereas the M2 coordination changes from sixfold (296 K) to sevenfold (1200 K) and to sixfold (1300 K) because of the bridging O3B moving out and O3B′ moving into the coordination sphere ($r \leq 3.0$ Å) at elevated temperatures. At 1300 K, the highly distorted M2 octahedron shares two edges with SiA and SiB, rather than one with SiA at 296 K, and the structure has all features of the high-temperature orthopyroxene phase predicted by Pannhorst (1979), which, in fact, is a transitional structural state between orthopyroxene and the so-called protoenstatite. On the basis of the configurations of the silicate chains in Mg- and Fe-rich orthopyroxenes at high temperature, an explanation is given as to why Mg-rich orthopyroxenes tend to transform to the protoenstatite structure with increasing temperature, whereas Fe-rich ones tend to transform to a clinopyroxene with space group $C2/c$. The anomalous behavior of the Fe-Mg order-disorder above 1200 K is attributed to the existence of the transitional state, particularly the changing charge distribution around the M2 site.

INTRODUCTION

Mg-rich orthopyroxene, $(Mg,Fe)_2Si_2O_6$, is a major constituent of the Earth's crust and the upper mantle. A knowledge of the response of the orthopyroxene structure to high temperature, especially the mechanisms of the phase transitions from orthopyroxene to other high-temperature polymorphs, so-called protoenstatite or clinopyroxene with space group $C2/c$, is of great geophysical importance in understanding the Earth's interior. Under ambient conditions, orthopyroxene crystallizes in the orthorhombic space group *Pbca*. Its crystal structure consists of two nonequivalent tetrahedral $(SiO_3)^{2-}$ chains, A and B, and two crystallographically distinct MO_6 octahedra, M1 and M2 (M = Mg, Fe, etc.). Both A and B chains running parallel to c are kinked, and the kinking angles (∠O3-O3-O3, O3 being the bridging O atom) deviate considerably from 180°, the characteristic value for a fully extended chain. Throughout the orthopyroxene compositional range ($Mg_2Si_2O_6$-$Fe_2Si_2O_6$), the B chain is kinked ~20° more than the A chain. The octahedral M1 site is smaller and nearly regular, whereas the M2 site is larger and more distorted. In orthopyroxenes, the cation ordering is very strong, with Mg preferring the M1 site and Fe the M2 site (Ghose, 1965). Because of its importance in the determination of cooling rates of host rocks and the excess thermodynamic properties of the orthopyroxene solid solution, the intracrystalline Fe-Mg distribution in orthopyroxenes has been extensively studied (e.g., Ghose and Hafner, 1967; Virgo and Hafner, 1969; Saxena and Ghose, 1971; Besancon, 1981; Anovitz et al., 1988; Saxena et al., 1989; Sykes-Nord and Molin, 1993; Yang and Ghose, 1994a).

At high temperature, orthopyroxene transforms reconstructively to different phases depending on the chemical composition. Enstatite, $Mg_2Si_2O_6$, transforms to the "protoenstatite" with the space group *Pbcn* at ~1300 K (e.g., Smyth, 1974; Murakami et al., 1982), whereas ferrosilite, $Fe_2Si_2O_6$, transforms reversibly and topotactically to clinoferrosilite with the space group $C2/c$ at ~1300

0003–004X/95/0102–0009$02.00

K (Sueno and Kimata, 1981; Sueno and Prewitt, 1983; Sueno et al., 1984, 1985). Intermediate orthopyroxenes with X_{Fe} = Fe/(Fe + Mg) > 13% also transform to $C2/c$ clinopyroxenes (Smyth, 1969; Sueno et al., 1985), but the transition is irreversible and nontopotactic, and the transition temperature decreases from ~1500 to 1250 K with increasing Fe content. Upon cooling, the $C2/c$ phase, sometimes referred to as high clinopyroxene, undergoes a reversible and displacive transition to clinopyroxene with the space group $P2_1/c$, or a low clinopyroxene (Smyth, 1969; Smyth and Burnham, 1972; Sueno and Kimata, 1981; Sueno and Prewitt, 1983; Sueno et al., 1985), whereas protoenstatite transforms to either $P2_1/c$ clinopyroxene or a mixture of $P2_1/c$ clinopyroxene and orthopyroxene, depending on the cooling rates (Smyth, 1974; Lee and Heuer, 1987; Schrader et al., 1990; Boysen et al., 1991). Various mechanisms have been proposed for the pyroxene phase transitions (Brown et al., 1961; Sadanaga et al., 1969; Coe, 1970; Smyth, 1974; Coe and Kirby, 1975; Sueno and Prewitt, 1983) and reviewed by Smith (1969), Pannhorst (1979), Sueno and Prewitt (1983) and Lee and Heuer (1987).

Orthopyroxene structures as a function of temperature have been reported on an intermediate orthopyroxene, $(Mg_{0.30}Fe_{0.68}Ca_{0.02})_2Si_2O_6$, up to 1123 K (Smyth, 1973) and on pure ferrosilite, $Fe_2Si_2O_6$, up to 1253 K (Sueno et al., 1976). Mg-rich orthopyroxenes are more common in the Earth and meteorites than Fe-rich ones, but no high-temperature structural data on Mg-rich orthopyroxenes are available so far. A thermal expansion study of the unit-cell dimensions of orthopyroxenes revealed that the thermal behavior of Mg-rich orthopyroxenes ($X_{Fe} \leq 20\%$) is quite different from that of Fe-rich ones ($X_{Fe} \geq 40\%$) (Yang and Ghose, 1994b). Sykes-Nord and Molin (1993) suggested that there is a gap in the activation energies for the Fe-Mg ordering between Mg-rich and Fe-rich orthopyroxenes. Furthermore, Ohashi and Finger (1973) and Pannhorst (1979) predicted the existence of a high-temperature orthorhombic phase and possibly a new structure type, which has the same space group as orthopyroxene. Using in-situ high-temperature X-ray precession photography, Murakami et al. (1982) reported an intermediate phase between enstatite and protoenstatite at 1273 K, which is characterized by an a dimension similar to that of orthopyroxene, but the intensity distribution of the strong reflections similar to that of protoenstatite. Presumably, the silicate chains in this phase are stretched and are similar to those in protoenstatite, but the basic stacking sequence of the orthopyroxene structure is still maintained. To clarify some of these questions, we have undertaken an in-situ high-temperature single-crystal X-ray diffraction study of the crystal structures and site occupancies of a synthetic $(Mg_{0.75}Fe_{0.25})_2Si_2O_6$ orthopyroxene at 296, 1000, 1100, 1200, and 1300 K. We report a transitional structural state between orthopyroxene and protoenstatite at 1300 K. The anomalous intracrystalline Fe-Mg equilibrium distribution observed above 1200 K is due to the existence of the transitional state. The results reported in this paper are a part of our systematic in-situ high-temperature studies of the orthopyroxene structures and site occupancies within the compositional range $Mg_2Si_2O_6$-$Fe_2Si_2O_6$ up to 1300 K (Yang, 1994).

Experimental methods

Sample

To avoid complications due to the presence of minor elements in natural orthopyroxenes (Ca, Al, Mn, Cr, Ti, etc.) and their influence on the crystal structure and the intracrystalline Fe-Mg distribution, a synthetic single crystal with the chemical composition $(Mg_{0.75}Fe_{0.25})_2Si_2O_6$ was chosen for the study, designated here as Fs_{25} for simplicity (Fs = ferrosilite, $Fe_2Si_2O_6$). The sample was synthesized hydrothermally at 1253 K and 20 kbar in a piston-cylinder apparatus by D. H. Lindsley and H. Yang at SUNY, Stony Brook, following the crystal growth procedure described by Turnock et al. (1973). The crystal used for the X-ray diffraction study was chemically analyzed in a JEOL 733 electron microprobe at the University of Washington with a 15-keV accelerating voltage and a 25-nA beam current measured on the Faraday cup with the result SiO_2, 55.62; MgO, 27.99; FeO, 16.55 (wt%). The compositional variability of the crystal examined by the electron microprobe showed that the crystal was quite homogeneous.

Data collection and structure refinement

The crystal used for this study is from among those reported on by Yang and Ghose (1994a), who described details of X-ray intensity data collection and structure refinement. In addition to the data collected at 1000, 1100, 1200, and 1300 K by Yang and Ghose (1994a), we collected intensity data at 296 K for structure refinement and determined unit-cell dimensions at 296, 600, and 800 K on the same crystal. The reader is referred to Yang and Ghose (1994a) for further information concerning methods.

Heating durations, unit-cell dimensions, final weighted and unweighted discrepancy indices (R_w and R), and site occupancies are given in Table 1. Atomic positional coordinates and anisotropic and isotropic thermal vibrational parameters from final cycles of refinements are presented in Table 2, and selected interatomic distances, uncorrected for thermal vibrations, and angles are presented in Tables 3 and 4, respectively. Atomic positional coordinates and isotropic thermal vibrational parameters from cooling experiments are very similar to those from the heating experiments and are not reported.

Results and discussion

Thermal expansion of unit-cell parameters

The unit-cell dimensions and volumes of the Fs_{25} orthopyroxene as a function of temperature are shown in Figure 1. From 296 to 1200 K, the a and c dimensions increase with a positive curvature, whereas, the b dimension increases nearly linearly. However, there is a sharp

TABLE 1. Crystal data and other relevant information on the $En_{75}Fs_{25}$ orthopyroxene at various temperatures

T (K)	Heating (h)	a (Å)	b (Å)	c (Å)	Total refs.	Refs. $>3\sigma_I$	R_w	R	Fe^{M1}	Fe^{M2}
					On heating					
296		18.2747(21)	8.8729(9)	5.1988(5)	1838	1086	0.042	0.034	0.093(3)	0.405
600		18.3177(20)	8.9120(10)	5.2141(5)						
800		18.3513(20)	8.9347(10)	5.2279(5)						
1000	36	18.3878(21)	8.9577(10)	5.2441(5)	1859	702	0.036	0.034	0.084(3)	0.414
1100	24	18.4105(19)	8.9691(9)	5.2540(5)	1865	656	0.036	0.035	0.099(4)	0.399
1200	4	18.4317(21)	8.9822(10)	5.2647(5)	1878	605	0.042	0.037	0.115(5)	0.383
1300	2	18.5132(28)	8.9809(13)	5.3243(8)	1883	518	0.042	0.038	0.119(5)	0.379
					On cooling					
1000	36	18.3877(29)	8.9585(14)	5.2432(8)	1853	707	0.042	0.039	0.084(4)	0.414
1100	24	18.4093(31)	8.9687(14)	5.2530(8)	1863	609	0.037	0.035	0.097(4)	0.401
1200	4	18.4302(31)	8.9825(15)	5.2643(9)	1874	570	0.039	0.037	0.115(4)	0.383
1300	2	18.5141(35)	8.9800(16)	5.3255(10)	1888	522	0.043	0.035	0.121(4)	0.377

increase in the expansion rate of the *a* and *c* dimensions and a slight decrease in the *b* dimension from 1200 to 1300 K, implying that marked structural changes occur in this temperature range. Because the silicate chains are parallel to **c**, the large increase in the *c* dimension indicates a pronounced straightening of the silicate chains between 1200 and 1300 K. Since the SiO_4 tetrahedra in pyroxenes do not expand significantly with increasing temperature (Cameron and Papike, 1981), the considerable increase in the *a* dimension suggests a large expansion in the M-O bonds along **a**. The slight decrease in the *b* dimension from 1200 to 1300 K is closely related to the straightening of the silicate chains and the shortening of some of the M2-O3 bonds in the structure (Boysen et al., 1991; Yang and Ghose, 1994b).

Structural variations with temperature

The previous in-situ high temperature X-ray diffraction studies of the orthopyroxene structure show that the silicate B chain unkinks faster than the A chain with increasing temperature (Smyth, 1973; Sueno et al., 1976; Yang, 1994). However, we observed a drastic increase in the rate of unkinking of the B chain above 1200 K, such that at 1300 K, the O3-O3-O3 angle of the B chain (173.1°) is larger (albeit with a different skew) than that of the A chain (170.8°) (Fig. 2), i.e., the B chain has become straighter than the A chain. For comparison, the data reported by Sueno et al. (1976, 1984) on ferrosilite and by Yang and Ghose (in preparation) on enstatite are also plotted in Figure 2. It can be seen that the kinking angles of the A and B chains in the Fs_{25} orthopyroxene approach each other at a much faster rate as temperature increases than those in enstatite and ferrosilite. In addition to the striking changes in the kinking angles of the silicate chains, the Si-O bond distances and angles within two silicate tetrahedra (SiA and SiB) also change considerably (Tables 3 and 4). From 296 to 1200 K, all Si-O bond distances (uncorrected for thermal vibrations) decrease at different rates; but from 1200 to 1300 K, the Si-O2 and SiA-O1A distances begin to increase, while the others continue to decrease. Compared with the Si-O bond distances within the SiA tetrahedron, those within the SiB tetrahedron appear to be more sensitive to the temperature variation. For instance, from 1200 to 1300 K, the average SiB-O3B distance decreases far more (0.015 Å) than the average SiA-O3A distances (0.003 Å), and the SiB-O2B distance increases more (0.011 Å) than the SiA-O2A distance (0.005 Å). Owing to the significant changes in the B chains, the configurations of the A and B chains become very similar at 1300 K in terms of the out-of-plane tilting angles (Cameron et al., 1973), shapes and sizes of the SiO_4 tetrahedra, and the kinking angles of the silicate chains (Tables 3 and 4).

To gain an insight into the effects of the thermally activated tetrahedral libration on the apparent shortening of the Si-O distances with increasing temperature, we applied the rigid-body thermal vibration analysis to the β_{ij} data using the program THMA13 (Trueblood, 1978), which is the formalism proposed by Schomaker and Trueblood (1968). The Si-O bond distances corrected for the thermal librations of the silicate tetrahedra, with allowance for internal vibrations, are given in Table 5. Listed in Table 6 are the rigid-body librational eigenvalues (L_i) and eigenvectors for two silicate tetrahedra in the Fs_{25} orthopyroxene. Although most Si-O bond lengths corrected for thermal librations at 1300 K are very similar to the corresponding ones at 1200 K, the decrease in the SiB-O3B′ distance and the increase in the Si-O2 distances from 1200 to 1300 K are significant and indicate an approaching phase transition. Note that, with the thermal vibrational corrections, the mean SiA-O and SiB-O bond distances are nearly unchanged between 296 and 1200 K. The thermal librational motion of the SiB tetrahedron increases faster than that of the SiA tetrahedron: at 296 K, the SiA tetrahedron exhibits larger librational motion (L_1 = 8.1°²) than the SiB tetrahedron (5.2°²), similar to the results of Ghose et al. (1986) for enstatite; but at 1300 K, the SiB tetrahedron shows considerably larger librational motion (77.3°²) than the SiA tetrahedron (48.0°²) (Table 6). The substantial increase in the degree of the thermal libration of the SiB tetrahedron above 1200 K is apparently responsible for the faster rate of unkinking of the B chain (Tables 3 and 4). The principal librational axis for the SiA tetrahedron is parallel to **a** throughout

TABLE 2. Atomic positional coordinates and anisotropic and isotropic displacement parameters of the $En_{75}Fs_{25}$ orthopyroxene at various temperatures

T (K)		296	1000	1100	1200	1300
Mg1	x	3757(1)	3751(1)	3751(1)	3750(1)	3746(1)
	y	6543(1)	6521(1)	6518(1)	6511(1)	6502(2)
	z	8702(1)	8803(2)	8826(2)	8884(3)	9084(5)
	β_{11}	4(1)	12(1)	14(1)	16(1)	18(1)
	β_{22}	14(1)	47(1)	54(1)	66(2)	70(3)
	β_{33}	41(2)	111(4)	136(4)	153(5)	170(8)
	β_{12}	0(1)	0(1)	0(1)	0(1)	0(1)
	β_{13}	−1(1)	−5(1)	−8(1)	−6(1)	−5(2)
	β_{23}	0(1)	0(2)	2(2)	2(3)	3(6)
	B_{iso}	0.494	1.490	1.740	2.043	2.196
Mg2	x	3776(1)	3769(1)	3767(1)	3763(1)	3753(1)
	y	4848(1)	4854(1)	4856(1)	4863(1)	4870(2)
	z	3640(1)	3754(1)	3784(2)	3853(2)	4080(5)
	β_{11}	5(1)	18(1)	21(1)	24(1)	27(1)
	β_{22}	19(1)	66(1)	74(1)	88(2)	103(3)
	β_{33}	51(2)	162(3)	182(4)	222(5)	237(8)
	β_{12}	−1(1)	−4(1)	−3(1)	−5(1)	−4(1)
	β_{13}	−4(1)	−17(1)	−16(1)	−21(1)	−17(2)
	β_{23}	1(1)	6(1)	7(2)	8(3)	3(6)
	B_{iso}	0.635	2.150	2.443	2.886	3.211
SiA	x	2717(1)	2719(1)	2720(1)	2721(1)	2717(1)
	y	3408(1)	3400(1)	3397(1)	3396(1)	3391(3)
	z	521(1)	592(2)	610(2)	656(2)	829(4)
	β_{11}	3(1)	8(1)	9(1)	10(1)	13(1)
	β_{22}	14(1)	37(1)	42(1)	49(1)	53(3)
	β_{33}	40(2)	97(3)	100(3)	117(4)	137(7)
	β_{12}	0(1)	−2(1)	−3(1)	−2(1)	−3(1)
	β_{13}	0(1)	0(1)	0(1)	0(1)	−3(2)
	β_{23}	0(1)	−4(2)	0(2)	−4(2)	−2(4)
	B_{iso}	0.454	1.154	1.243	1.444	1.638
SiB	x	4737(1)	4747(1)	4750(1)	4756(1)	4773(1)
	y	3366(1)	3371(1)	3376(1)	3380(1)	3391(3)
	z	7959(1)	7887(1)	7864(2)	7807(2)	7612(4)
	β_{11}	3(1)	8(1)	9(1)	10(1)	11(1)
	β_{22}	13(1)	38(1)	43(1)	49(1)	61(3)
	β_{33}	41(2)	96(3)	111(3)	136(4)	138(7)
	β_{12}	0(1)	2(1)	0(1)	1(1)	2(1)
	β_{13}	−1(1)	−3(1)	−4(1)	−4(1)	−2(2)
	β_{23}	0(1)	2(1)	0(2)	0(2)	5(5)
	B_{iso}	0.450	1.136	1.282	1.519	1.738
O1A	x	1836(1)	1844(1)	1846(1)	1850(2)	1849(3)
	y	3383(2)	3389(3)	3394(3)	3392(4)	3410(8)
	z	401(3)	502(5)	530(5)	594(7)	788(11)
	β_{11}	3(1)	8(1)	10(1)	9(1)	11(1)
	β_{22}	18(2)	61(3)	60(4)	78(5)	88(9)
	β_{33}	61(6)	133(9)	164(10)	164(12)	181(22)
	β_{12}	−1(1)	−3(1)	0(1)	0(2)	0(4)
	β_{13}	3(1)	2(2)	1(2)	3(2)	−9(5)
	β_{23}	−1(3)	4(6)	−6(6)	0(8)	7(14)
	B_{iso}	0.566	1.534	1.704	1.861	2.215
O1B	x	5626(1)	5627(1)	5627(1)	5631(2)	5642(3)
	y	3387(2)	3403(3)	3405(3)	3424(4)	3431(8)
	z	7968(4)	7898(5)	7888(5)	7829(7)	7637(14)
	β_{11}	3(1)	8(1)	9(1)	12(1)	13(1)
	β_{22}	18(2)	61(3)	71(4)	70(5)	82(9)
	β_{33}	59(6)	151(9)	167(10)	187(12)	265(27)
	β_{12}	0(1)	−3(1)	−2(1)	−5(2)	−4(4)
	β_{13}	0(1)	−7(2)	−6(2)	−4(3)	−3(6)
	β_{23}	1(3)	7(5)	8(6)	−3(8)	16(17)
	B_{iso}	0.570	1.598	1.818	2.033	2.446
O2A	x	3112(1)	3112(1)	3111(1)	3115(2)	3126(4)
	y	5008(2)	4985(3)	4976(3)	4965(4)	4951(8)
	z	496(4)	624(6)	654(6)	726(7)	918(13)
	β_{11}	5(1)	15(1)	19(1)	21(1)	28(2)
	β_{22}	19(2)	50(3)	58(4)	65(5)	65(8)
	β_{33}	68(6)	172(10)	192(12)	218(15)	251(27)
	β_{12}	−2(1)	−7(1)	−12(2)	−15(2)	−13(4)
	β_{13}	−3(1)	−5(2)	−6(2)	−10(3)	1(7)
	β_{23}	4(3)	4(6)	9(7)	10(9)	2(15)
	B_{iso}	0.715	1.888	2.205	2.486	2.832
O2B	x	4334(1)	4338(1)	4342(1)	4347(2)	4363(4)
	y	4841(2)	4845(3)	4853(3)	4870(4)	4938(8)
	z	6927(4)	6996(5)	7012(6)	7052(8)	7223(15)
	β_{11}	5(1)	17(1)	17(1)	20(1)	24(2)

TABLE 2.—*Continued*

T (K)		296	1000	1100	1200	1300
	β_{22}	17(2)	47(3)	49(4)	69(5)	77(10)
	β_{33}	67(6)	142(9)	196(11)	224(14)	244(27)
	β_{12}	2(1)	11(1)	11(1)	14(2)	19(4)
	β_{13}	−2(1)	−7(2)	−1(3)	−3(3)	6(6)
	β_{23}	0(3)	8(5)	15(6)	20(9)	6(16)
	B_{iso}	0.683	1.810	2.046	2.502	2.884
O3A	x	3027(1)	3023(1)	3023(1)	3022(2)	3018(4)
	y	2267(2)	2308(3)	2320(4)	2339(5)	2380(10)
	z	−1703(4)	−1688(5)	−1675(6)	−1658(8)	−1556(11)
	β_{11}	5(1)	11(1)	15(1)	17(1)	15(2)
	β_{22}	29(2)	80(4)	94(5)	117(6)	140(13)
	β_{33}	52(6)	124(10)	137(11)	141(14)	210(24)
	β_{12}	0(1)	2(1)	−2(1)	4(2)	−2(4)
	β_{13}	0(1)	−3(2)	0(2)	−4(3)	0(5)
	β_{23}	−11(3)	−39(5)	−47(6)	−59(9)	−80(17)
	B_{iso}	0.746	1.827	2.240	2.587	3.123
O3B	x	4476(1)	4483(1)	4489(1)	4490(2)	4508(5)
	y	1984(2)	2058(3)	2084(4)	2136(5)	2405(11)
	z	5982(3)	5831(5)	5780(6)	5664(8)	5190(15)
	β_{11}	5(1)	14(1)	15(1)	13(1)	22(3)
	β_{22}	19(2)	68(4)	81(4)	117(7)	186(17)
	β_{33}	44(6)	147(10)	178(12)	249(17)	308(32)
	β_{12}	−1(1)	−4(1)	−3(1)	−6(2)	−10(6)
	β_{13}	−2(1)	6(2)	5(2)	4(3)	7(8)
	β_{23}	−3(3)	−37(5)	−47(6)	−75(9)	−170(24)
	B_{iso}	0.623	1.937	2.240	2.787	4.005

Note: atomic positional coordinates and anisotropic displacement parameters are shown times 10^4; isotropic displacement parameters are shown in squared ångströms.

the temperature range (296–1300 K), whereas that for the SiB tetrahedron is parallel to **c** between 296 and 1000 K and changes to **a** between 1000 and 1300 K.

In general, topologic changes produced by increasing temperature are expected to be similar to those produced by substitution of larger cations for smaller ones. However, numerous exceptions have been found for clinopyroxenes (Cameron and Papike, 1981). An obvious exception also exists in orthopyroxenes: with increasing Fe content, the silicate A chain straightens nearly twice as fast as the B chain (Cameron and Papike, 1981), whereas with increasing temperature, the results reported in the present and previous studies (Smyth, 1973; Sueno et al., 1976) show that the B chain straightens about twice as fast as the A chain. The higher rate of unkinking of the A chain with increasing Fe content may be related to the increasing mismatch between the M2 octahedron and the SiA tetrahedron, caused by the parity violation in the A chain (the M2 octahedron shares an edge with the SiA tetrahedron). On the other hand, the greater rate of straightening of the B chain with increasing temperature may arise from the differential thermal expansion between the silicate tetrahedra and the MO_6 octahedra (see below) and the fact that the B chain becomes more flexible at higher temperatures, as indicated by the higher rate of increase of thermal libration of the SiB tetrahedron than that of the SiA tetrahedron.

From 296 to 1300 K, the M1 octahedron remains nearly regular, and all individual M1-O bond lengths increase smoothly with temperature (Table 3). By contrast, the M2 octahedron undergoes significant changes in shape and size as a function of temperature. With increasing temperature, the four relatively short M2-O bond distances (M2-O1A, M2-O2A, M2-O1B, and M2-O2B) do not change significantly, but the two relatively long M2-O3 distances increase considerably, M2-O3B increasing much faster than M2-O3A. As a result of the pronounced straightening of the silicate B chain from 1200 to 1300 K, the M2 coordination (within a radius of 3.0 Å) changes from six at 296 K to seven at 1200 K and back to six at 1300 K (Fig. 3). The marked straightening of the B chain from 1200 to 1300 K results in a sharp increase in the M2-O3B bond from 2.80 to 3.23 Å and a corresponding decrease in the M2-O3B′ bond from 2.95 to 2.67 Å. A similar switching of the bridging O3B atoms coordinated with the M2 cation has been reported for other Fe-bearing orthopyroxenes (Smyth, 1973; Sueno et al., 1976; Yang, 1994). However, the temperature at which the O3B atoms start switching coordination appears to increase with increasing Mg content: ~950 K for pure ferrosilite (Sueno et al., 1976), ~1040 K for intermediate orthopyroxene (Smyth, 1973), and ~1230 K for the Fs_{25} orthopyroxene. This trend is parallel to that at which orthopyroxene transforms to protoenstatite or *C2/c* clinopyroxene as a function of the Mg content. This similarity suggests that the thermal behavior of the M2 site configuration, particularly the bonding of the M2 cation with the bridging O3 atoms, has a strong influence on the nature of the phase transition in orthopyroxenes. Because of the switching of the bridging O3B atoms, the M2 octahedron at 1300 K not only shares an edge with the SiA tetrahedron, but also one with the SiB tetrahedron (Fig. 4). Energetically, such a polyhedral configuration is unstable because of the strong parity violation. This may

TABLE 3. Selected bond distances* (Å) within the coordination polyhedra and other geometric parameters in the $En_{75}Fs_{25}$ orthopyroxene at various temperatures

T (K)	296	1000	1100	1200	1300
SiA-O1A	1.612(2)	1.608(2)	1.610(3)	1.605(4)	1.611(4)
-O2A	1.593(2)	1.594(3)	1.589(3)	1.586(4)	1.591(5)
-O3A	1.639(2)	1.643(3)	1.640(3)	1.641(4)	1.640(5)
-O3A′	1.662(2)	1.658(3)	1.661(3)	1.656(4)	1.651(5)
Av.	1.626	1.626	1.625	1.622	1.623
TV (Å³)**	2.18	2.18	2.18	2.17	2.17
TQE	1.009	1.008	1.008	1.008	1.007
TAV	35.80	31.82	31.99	32.22	28.15
Tilting (°)	3.95	4.21	4.13	4.39	5.63
SiB-O1B	1.625(2)	1.617(2)	1.615(3)	1.612(4)	1.609(4)
-O2B	1.595(2)	1.590(3)	1.587(3)	1.587(4)	1.598(5)
-O3B	1.670(2)	1.668(3)	1.664(3)	1.661(5)	1.650(6)
-O3B′	1.672(2)	1.664(3)	1.657(3)	1.649(4)	1.630(6)
Av.	1.640	1.635	1.631	1.627	1.621
TV (Å³)	2.24	2.23	2.21	2.20	2.17
TQE	1.005	1.005	1.005	1.005	1.005
TAV	19.60	19.14	19.34	17.43	22.81
Tilting (°)	6.64	6.92	6.97	6.76	6.38
M1-O1A	2.032(2)	2.051(3)	2.054(3)	2.058(4)	2.070(5)
-O1A′	2.150(2)	2.190(3)	2.201(3)	2.212(4)	2.233(5)
-O1B	2.065(2)	2.074(3)	2.071(3)	2.072(4)	2.078(5)
-O1B′	2.168(2)	2.224(3)	2.232(3)	2.250(4)	2.258(5)
-O2A	2.028(2)	2.045(3)	2.056(3)	2.059(4)	2.057(5)
-O2B	2.060(2)	2.078(3)	2.079(3)	2.078(4)	2.057(5)
Av.	2.084	2.110	2.116	2.122	2.125
OQE	1.008	1.009	1.009	1.010	1.012
OAV	25.40	27.45	27.23	28.31	32.24
M2-O1A	2.134(2)	2.143(3)	2.139(3)	2.140(4)	2.114(5)
-O1B	2.084(2)	2.102(3)	2.108(3)	2.097(4)	2.101(5)
-O2A	2.040(2)	2.042(3)	2.043(3)	2.037(4)	2.046(5)
-O2B	1.990(2)	1.996(3)	2.000(3)	1.999(4)	2.025(6)
-O3A	2.329(2)	2.386(3)	2.397(3)	2.419(4)	2.471(6)
-O3B	2.488(2)	2.648(3)	2.700(3)	2.800(5)	3.226(6)
-O3B′	3.095(2)	3.030(3)	3.008(4)	2.949(5)	2.668(7)
Av. of 6	2.177	2.219	2.231	2.248	2.237
Av. of 7	2.308	2.335	2.342	2.348	2.379
OQE	1.060	1.069	1.072	1.083	1.125
OAV	165.8	180.0	185.4	201.5	256.3

* Uncorrected for the thermal librations.

** TV = tetrahedral volume; TQE = tetrahedral quadratic elongation; TAV = tetrahedral angle variance; OQE = octahedral quadratic elongation; OAV = octahedral angle variance (Robinson et al., 1971).

explain why the protoenstatite and *C2/c* clinopyroxene phases are unquenchable, since the M2 octahedra in both structures share two edges with the adjacent SiO_4 tetrahedra (Smyth and Burnham, 1972; Murakami et al., 1982, 1984, 1985; Sueno et al., 1984). The pronounced change in the configuration of the M2 octahedron is also likely to be responsible for the anomalous temperature dependence of the Fe-Mg order-disorder from 1200 to 1300 K, as illustrated by Yang and Ghose (1994a).

TABLE 4. Interatomic angles (°) within the tetrahedra in the $En_{75}Fs_{25}$ orthopyroxene at various temperatures

T (K)	296	1000	1100	1200	1300
O1A-SiA-O2A	117.7(1)	117.4(2)	117.0(2)	117.4(2)	117.4(3)
O1A- -O3A	111.7(1)	111.1(1)	111.0(2)	110.6(2)	109.5(3)
O1A- -O3A′	108.1(1)	108.4(2)	108.7(2)	108.8(2)	108.8(3)
O2A- -O3A	100.0(1)	100.3(2)	100.4(2)	100.4(2)	101.0(3)
O2A- -O3A′	111.7(1)	112.6(1)	112.4(2)	112.1(2)	111.1(3)
O3A- -O3A′	105.8(1)	106.4(1)	106.6(1)	106.8(2)	108.2(2)
O1B-SiB-O2B	117.0(1)	117.4(2)	117.5(2)	117.1(2)	117.5(3)
O1B- -O3B	107.2(1)	107.8(1)	107.7(2)	108.5(2)	109.3(3)
O1B- -O3B′	106.6(1)	107.0(1)	106.6(2)	107.3(2)	108.6(3)
O2B- -O3B	105.3(1)	104.2(2)	105.0(2)	104.9(2)	102.5(3)
O2B- -O3B′	109.7(1)	109.1(2)	109.3(2)	108.9(2)	109.7(3)
O3B- -O3B′	111.1(1)	110.6(1)	110.6(1)	110.1(1)	108.8(2)
O3A-O3A-O3A	161.9(2)	165.1(3)	166.0(3)	167.5(4)	170.8(5)
O3B-O3B-O3B	141.2(2)	146.4(2)	148.4(3)	152.2(4)	173.1(6)
SiA-O3A-SiA	136.5(2)	137.7(2)	137.9(2)	138.7(3)	141.3(4)
SiB-O3B-SiB	130.8(2)	132.7(3)	134.3(3)	136.1(4)	142.7(5)

Atomic thermal vibrations

Isotropic displacement factors (B_{iso}) for the four cations (M1, M2, SiA, and SiB) and the six O atoms all increase nonlinearly at elevated temperatures, similar to those reported for intermediate orthopyroxene (Smyth, 1973) but different from those for pure ferrosilite (Sueno et al., 1976); in the latter case, the B_{iso} values of some atoms vary linearly with temperature. Si atoms have the smallest isotropic displacement factors between 296 and 1300 K, attributable to the strong tetrahedral bonds between Si and O atoms. B_{iso} of the M2 atom is always larger than that of the M1 atom, and the difference increases with increasing temperature. This behavior stems from the fact that the M2 site is larger, more distorted, and more flexible than the M1 site (Table 3). Among six O atoms, the B_{iso} factors of the O3 atoms increase fastest and become the largest as temperature increases, and those of the O1

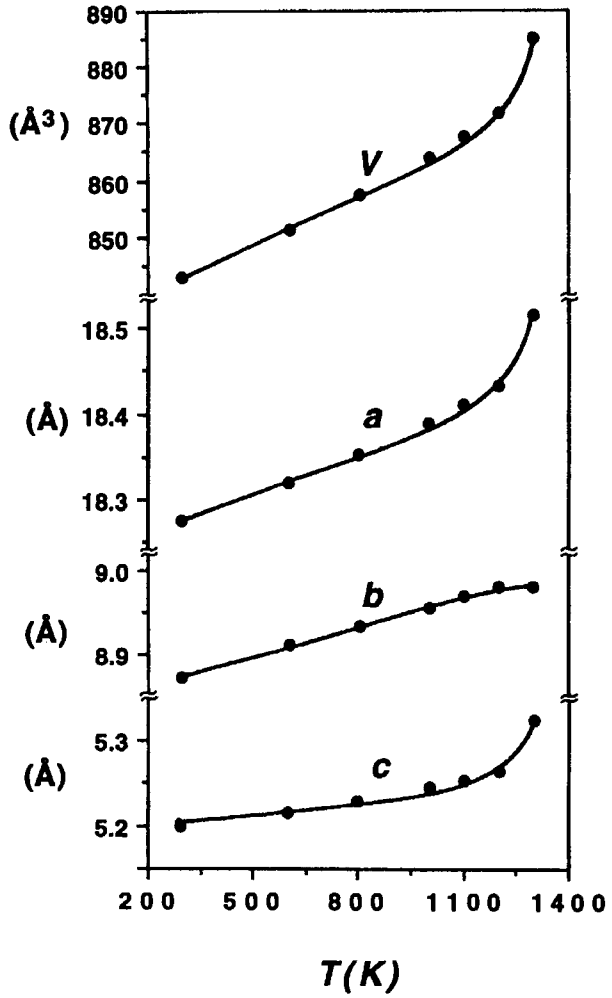

Fig. 1. Unit-cell dimensions of the $En_{75}Fs_{25}$ orthopyroxene as a function of temperature.

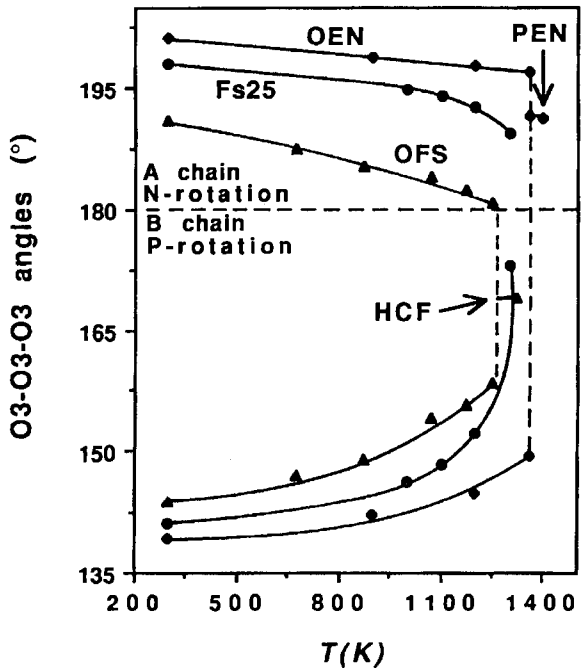

Fig. 2. Kinking angles (°) (∠O3-O3-O3) for the silicate A and B chains in the $En_{75}Fs_{25}$ orthopyroxene as a function of temperature. The kinking angle of the A chain is plotted above 180° (360° − ∠O3A-O3A-O3A) and that of the B chain below 180°, in accordance with Sueno et al. (1976). Diamonds represent orthoenstatite (OEN) and protoenstatite (PEN) (Yang and Ghose, in preparation), circles the $En_{75}Fs_{25}$ orthopyroxene (this study), and triangles orthoferrosilite (OFS) and high clinoferrosilite (HCF) (Sueno et al., 1976, 1984).

atoms increase most slowly and are the smallest. The high rates of increase of the B_{iso} parameters of the O3 atoms reflect their role as pivotal points during the unkinking of the silicate chains associated with strong tetrahedral librations. B_{iso} of the O3B atom increases much faster than that of the O3A atom from 296 to 1300 K because of the higher rate of straightening of the B chain and the increasing amplitude of libration of the SiB tetrahedron. These phenomena, coupled with the higher rate of increasing thermal displacements of the M2 atom, play an important role in the phase transition from *Pbca* to *Pbcn* or *C2/c* structures.

The magnitudes and orientations of the major axes of the atomic thermal vibrational ellipsoids in the Fs_{25} orthopyroxene at 296, 1000, 1100, 1200, and 1300 K are presented in Table 7.[1] The behavior of the atomic thermal vibrational ellipsoids in the Fs_{25} orthopyroxene is very similar to that described by Smyth (1973) for an intermediate orthopyroxene. Figure 3 shows the thermal vibrational ellipsoids for the atoms forming the M2 polyhedron at 296, 1200, and 1300 K. A notable feature of Figure 3 is that the longest ellipsoidal axes of most atoms tend to lie in the **b**-**c** plane. This is also true for the M1, SiA, and SiB atoms. Such a pattern is consistent with the fact that the thermal libration of the silicate tetrahedra around the **a** axis normal to the **b**-**c** plane is energetically the most favorable and thus the largest (Yang and Ghose, in preparation).

TABLE 5. Si-O bond distances* (Å) within the SiO_4 tetrahedra in the $En_{75}Fs_{25}$ orthopyroxene at various temperatures

T (K)	296	1000	1100	1200	1300
SiA-O1A	1.614	1.612	1.617	1.613	1.620
-O2A	1.596	1.602	1.600	1.599	1.606
-O3A	1.642	1.652	1.650	1.656	1.656
-O3A′	1.664	1.665	1.671	1.666	1.664
Av.	1.629	1.633	1.635	1.634	1.636
SiB-O1B	1.627	1.625	1.623	1.618	1.618
-O2B	1.596	1.598	1.597	1.599	1.618
-O3B	1.672	1.676	1.675	1.675	1.674
-O3B′	1.674	1.671	1.665	1.660	1.649
Av.	1.642	1.643	1.640	1.638	1.640

* Corrected for the thermal libration with allowance for internal vibration.

[1] Table 7 may be ordered as Document AM-95-577 from the Business Office, Mineralogical Society of America, 1130 Seventeenth Street NW, Suite 330, Washington, DC 20036, U.S.A. Please remit $5.00 in advance for the microfiche.

TABLE 6. Rigid-body librational eigenvalues (L_i) of SiO_4 tetrahedra in the Fs_{25} orthopyroxene at various temperatures

		SiA tetrahedron				SiB tetrahedron			
T(K)	L_i	Eigenvalue ($^{\circ 2}$)	Cos θ/a	Cos θ/b	Cos θ/c	Eigenvalue ($^{\circ 2}$)	Cos θ/a	Cos θ/b	Cos θ/c
296	1	8.09	0.9487	0.1571	−0.0757	5.21	−0.2790	0.1946	−0.9403
	2	5.67	−0.1252	0.3351	−0.9338	4.01	−0.6166	0.7147	0.3308
	3	1.61	−0.1213	0.9290	0.3495	2.21	0.7361	0.6722	−0.0793
1000	1	26.26	0.9394	0.1104	0.3246	21.27	−0.6326	−0.2156	0.7439
	2	16.47	0.3025	0.1786	−0.9363	13.46	0.1822	0.8921	0.4135
	3	0.47	−0.1614	0.9777	0.1344	11.01	−0.7528	0.3971	−0.5250
1100	1	29.47	0.9895	0.1404	−0.0354	30.63	0.8041	−0.1045	−0.5853
	2	21.79	−0.0314	−0.0306	−0.9990	13.02	0.0519	0.9930	−0.1059
	3	7.08	−0.1414	0.9896	−0.0258	10.19	0.5923	0.0548	0.8039
1200	1	41.93	0.8712	0.1911	0.4522	40.74	0.9570	−0.0790	−0.2790
	2	28.09	0.4123	0.2149	−0.8853	16.23	−0.2814	−0.0203	−0.9594
	3	−0.49	−0.2664	0.9577	0.1084	7.81	0.0701	0.9967	−0.0417
1300	1	48.00	0.9920	0.1167	0.0474	77.33	0.9587	−0.1264	−0.2548
	2	26.44	0.0307	0.1406	−0.9896	26.69	−0.2375	0.1373	−0.9616
	3	6.74	−0.1222	0.9832	0.1359	7.37	0.1565	0.9824	0.1016

A transitional structural state

Using ideal coordination polyhedra, Pannhorst (1979) discussed structural relationships between pyroxenes and predicted the existence of a new high-temperature structure type, which has the same space group as orthopyroxene but differs from the orthopyroxene structure in two major respects: (1) the silicate A and B chains are similarly stretched and, (2) as a result of the straightening of the B chain, one M2-O3B bond is broken and a new M2-O3B bond formed, such that the M2 octahedron not only shares an edge with the SiA tetrahedron but also one with the SiB tetrahedron. On the basis of the high-temperature study of Smyth (1973) on the $En_{30}Fs_{70}$ orthopyroxene, Pannhorst (1979) considered the orthopyroxene structure at 1123 K to be characteristic of his proposed new structure type. He believed that the transformation from the orthopyroxene structure to the new structure type in the $En_{30}Fs_{70}$ orthopyroxene has taken place, although the B chain is still more kinked by 12.8° than the A chain. The structure of the Fs_{25} orthopyroxene we observed at 1300 K has all the features described by Pannhorst (1979) for the high-temperature orthopyroxene phase, although it is not the same as that determined by Smyth (1973). It is interesting to note that the intermediate phase found by Murakami et al. (1982) also has similarities with the transitional state we observed at 1300 K for the Fs_{25} orthopyroxene.

Is the structure of the Fs_{25} orthopyroxene at 1300 K a new structure type as proposed by Pannhorst (1979) or a transitional structural state between orthopyroxene and protoenstatite? Apart from changes in the stacking sequences, the structural changes associated with the *Pbca* to *Pbcn* or *C2/c* phase transitions are: (1) the two configurationally different silicate chains in orthopyroxene become identical in the high-temperature phases and (2) the two octahedrally coordinated M sites, on general positions with the site symmetry 1 in the ortho structure, move to special positions with the site symmetry 2 in the high-temperature polymorphs. The difference of the kinking angles between the A and B chains ($\Delta\theta$) (where θ

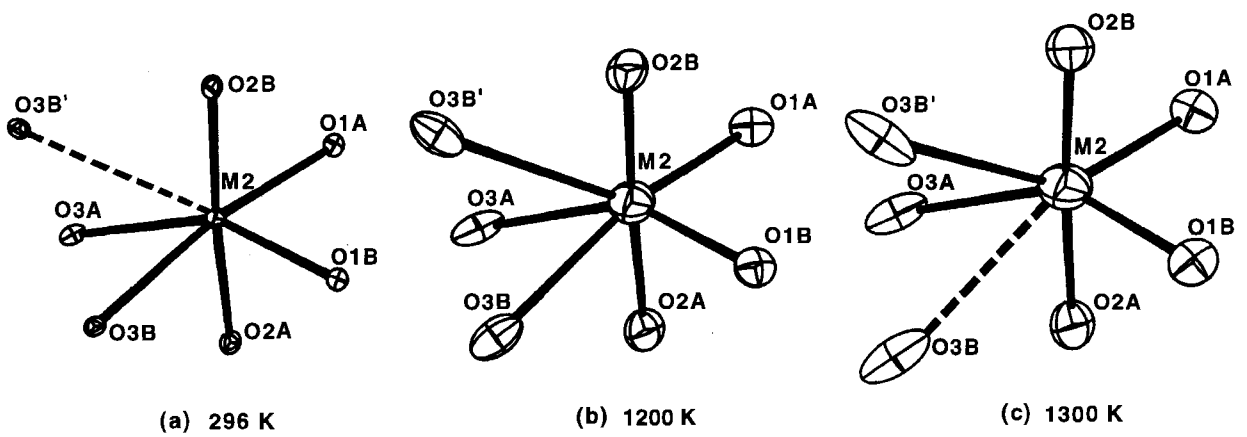

Fig. 3. Thermal vibration ellipsoids for atoms forming the M2 polyhedron in the $En_{75}Fs_{25}$ orthopyroxene: (a) at 296, (b) at 1200, and (c) at 1300 K. The ellipsoids represent 50% probability surfaces. The distances connected by solid lines are within 3.0 Å and the dashed lines beyond 3.0 Å.

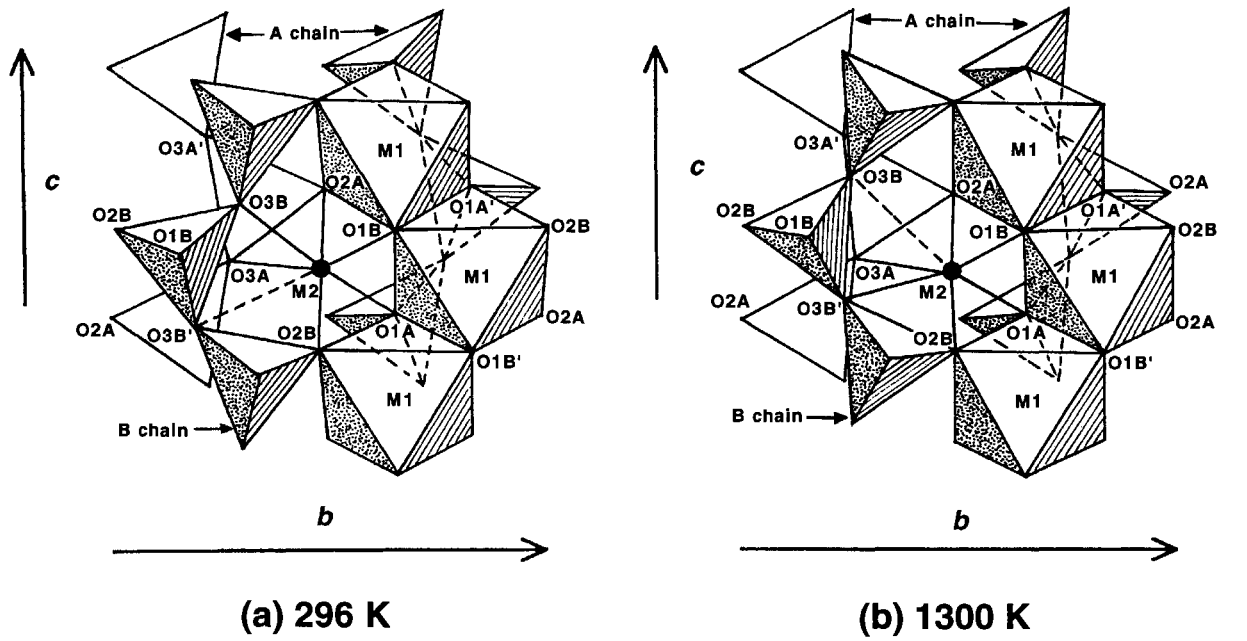

Fig. 4. Projection of a part of the $En_{75}Fs_{25}$ orthopyroxene structure along [100]: **(a)** at 296 K and **(b)** at 1300 K.

θ = ∠O3-O3-O3) can be taken as an order parameter to measure the structural variations with temperature (Fig. 5). It can be seen that the $\Delta\theta$ varies smoothly from 296 to 1300 K, similar to the behavior expected in a second-order phase transition. The fact that $\Delta\theta$ does not attain a zero value suggests that the structure of the Fs_{25} orthopyroxene at 1300 K is a transitional state, rather than a new structure type. On the other hand, the first-order *Pbca-Pbca* transition proposed by Pannhorst (1979) would require a discontinuity in the order parameter.

The transitional structure at 1300 K also has similarities with the high-temperature orthopyroxene structure proposed by Ohashi and Finger (1973). The space group of this hypothetical high-temperature orthopyroxene structure is also *Pbca* with regional symmetry that imposes extinction conditions for reflections that are not consistent with that space group. The high-temperature orthopyroxene phase is equivalent to a unit-cell scale twinning of the *C2/c* structure and is characterized by one type of silicate chain and the M1 and M2 cations on special positions. However, on the basis of their high-temperature study of ferrosilite, Sueno et al. (1976) concluded that Ohashi and Finger's (1973) hypothetical high-temperature phase cannot form in ferrosilite even if the O3-O3-O3 angles of both A and B chains become equivalent at high temperature. Their results show that variations of individual M1-O bond lengths with increasing temperature contradict the existence of the regional symmetry: two sets of Fe1-O bonds (Fe1 to O1A and O1B and Fe1 to O2A and O2B) become almost equivalent at 1253 K, but another set (Fe1-O1A′ and Fe1-O1B′) diverges with increasing temperature. The divergence violates the regional symmetry (C_2) in the high-temperature orthopyroxene phase. From Table 3, it can be seen that the separation between the M1-O1A′ and M1-O1B′ bond distances increases from 296 to 1200 K but decreases from 1200 to 1300 K, showing a tendency for the two bond lengths to approach each other. Such a tendency is found to be even stronger for Fe-rich orthopyroxenes (Yang, 1994). Thus, our data cannot preclude the possible

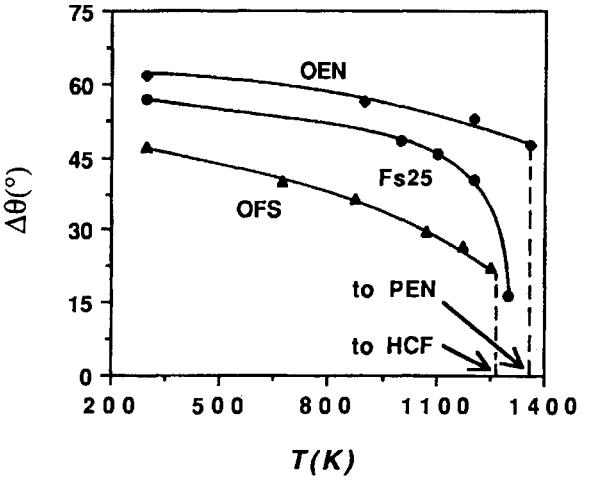

Fig. 5. Differences between the O3-O3-O3 angles of the A and B chains ($\Delta\theta$) as a function of temperature, which can be taken as an order parameter for a possible phase transition. OEN and PEN stand for orthoenstatite and protoenstatite (Yang and Ghose, in preparation), Fs_{25} the $En_{75}Fs_{25}$ orthopyroxene (this study), and OFS and HCF orthoferrosilite and high clinoferrosilite (Sueno et al., 1976, 1984).

existence of the hypothetical high-temperature orthopyroxene phase (Ohashi and Finger, 1973).

In their studies of the transformation from protoenstatite to clinoenstatite or enstatite, Schrader et al. (1990) and Boysen et al. (1991) noted a region of broadened and diffuse X-ray and neutron diffraction intensities, resulting from the development of extensive stacking faults. Similar results were also found in the transition from clinoenstatite to enstatite and from enstatite to protoenstatite by Pannhorst (1982) and Yang and Ghose (in preparation), respectively. According to Boysen et al. (1991), formation of stacking faults is energetically more favorable in the course of the transformation in enstatite because the nucleation at stacking faults helps trigger the transition. However, we did not observe significant diffuse intensities or broadening of X-ray reflections in the Fs_{25} crystal at 1300 K, nor in the $(Mg_{0.92}Mn_{0.08})_2Si_2O_6$ orthopyroxene at 1300 K, at which this crystal is also in a transitional state (Yang and Ghose, in preparation). Since no transitional state was found in enstatite prior to the phase transition to protoenstatite (Yang and Ghose, in preparation), we suggest that the phase transition mechanism for enstatite to protoenstatite is different from that in Fe-bearing pyroxenes.

Mechanisms for the phase transitions from *Pbca* to *Pbcn* or *C2/c*

The polymorphic transitions in pyroxenes are considered to be realized by the relative translation of unbroken silicate chains along **c** in the (100) plane, coupled with the breaking of some (Mg,Fe)-O bonds and retention of others (Brown et al., 1961; Sadanaga et al., 1969; Coe, 1970; Smyth, 1974; Pannhorst, 1979; Sueno and Prewitt, 1983). The differences among several mechanisms proposed for the phase transition from *Pbca* to *Pbcn* or *C2/c* are in the directions and the amounts of the relative displacements between the silicate chains and the M cations. In the Brown et al. (1961) model, the silicate chains and the M cations are displaced in the same directions by $\frac{2}{3}c$ and $\frac{1}{3}c$, respectively, whereas in the model of Sadanaga et al. (1969) and Coe (1970), the M cations are displaced as are those in the Brown et al. model, but the silicate chains are displaced in the opposite direction and the displacement is only $\frac{1}{3}c$. In other words, Sadanaga et al. (1969) and Coe (1970) assumed opposite displacement directions for the M cations and the silicate chains. A slight modification to the model of Sadanaga et al. (1969) and Coe (1970) was made by Smyth (1974), in which the displacements of the M cations are in the same direction as the silicate chains, and the M1 and M2 cations exchange their positions during the phase transition. This model successfully explains the coherent transformation in the pure end-member orthopyroxenes, in which both M1 and M2 sites are occupied only by Mg or Fe (Sueno and Kimata, 1981; Sueno et al., 1985). We observed small displacements of the silicate chains (~0.10 Å) and the M cations (~0.21 Å) in the same direction from 296 to 1300 K, which apparently favor Smyth's model. However, the structure of the Fs_{25} orthopyroxene at 1300 K still maintains the structural features of an orthopyroxene, whereas the martensitic or nearly martensitic transition from the orthopyroxene to its high-temperature phases involves large atomic displacements and considerable reconstruction of the structure. Hence, the small atomic displacements we observe cannot rule out any of these models.

Sueno et al. (1976) introduced the concept of P and N rotations of the silicate chains in pyroxenes to describe the structural configuration around the M2 site (see Fig. 3 of Sueno et al., 1976). In an N rotation, the basal triangles of the lateral tetrahedral chain point in a direction opposite to that of the octahedral faces to which they are joined through O2 atoms. In a P rotation, the triangular faces of the tetrahedra and octahedra joined through O2 are similarly oriented. The complete symbol for each M2 site includes two letters and a dot, the dot representing the position of the M2 cation. Thus, we have N·P for orthopyroxene (the A chain being N-rotated and the B chain P-rotated), N·N for protoenstatite and P·P for *C2/c* clinopyroxene. Besides the relative displacements of the silicate chains and M cations along **c**, an additional atomic rearrangement is needed for the *Pbca* to *Pbcn* or *C2/c* transition, which mainly involves the change of the skew of either the A or the B chain in terms of the P and N rotations, depending on to which polymorph it transforms. For the *Pbca* to *C2/c* transition, the skew of the A chain must be changed from N to P to achieve the P·P configuration, as in *C2/c* clinopyroxene, whereas for the *Pbca* to *Pbcn* transition, the skew of the B chain must be changed from P to N to achieve the N·N configuration as in protoenstatite. Although the total atomic displacements due to changing the skew of the silicate chains may be small compared with the relative displacements of the silicate chains and M cations, it may provide some clues as to why Mg-rich orthopyroxenes transform to the *Pbcn* structure, whereas Fe-rich ones transform to the *C2/c* structure. Given the same conditions, if the A chain is less kinked than the B chain at high temperature, it will be energetically more favorable for the A chain to reverse its skew (from N to P) than for the B chain, resulting in *C2/c* clinopyroxene (Fig. 2), but if the B chain is less kinked than the A chain at high temperature, there is a greater probability of the B chain changing its skew (from P to N) than the A chain, giving rise to the *Pbcn* protoenstatite structure.

If the above arguments are valid, then the Fs_{25} orthopyroxene is most likely to transform to protoenstatite above 1300 K because the B chain is ~3.0° less kinked than the A chain. The total estimated displacement for the B chain to be identical to the A chain by changing the skew of the B chain is ~0.37 Å, whereas that for the A chain to be identical to the B chain is ~0.50 Å. Therefore, energetically, it is more favorable for the B chain to change its skew (P rotation) than the A chain (N rotation). The very large thermal libration of the SiB tetrahedron at 1300 K suggests that the B chain is more flexible at higher temperatures, and, therefore, its skew is likely to

be changed from P to N. The above conclusion is supported by the comparison of X-ray intensities at 296 and 1300 K with those given by Murakami et al. (1982) for enstatite at ~296 and 1273 K, prior to the transition to protoenstatite at ~1300 K, which shows similar increases or decreases in the X-ray intensities of corresponding reflections. This inference is confirmed by the high-temperature experiment on the $(Mg_{0.92}Mn_{0.08})_2Si_2O_6$ orthopyroxene (Yang and Ghose, in preparation), which shows the transitional state between 1250 and 1385 K and transforms to protoenstatite at 1385 K.

The above argument can be applied to Fe-rich orthopyroxenes as well. Our high-temperature study of an orthopyroxene, $En_{25}Fs_{75}$, indicates that the A chain in this crystal is always less kinked than the B chain by at least 10°, even at a temperature (1200 K) near the phase transition point, which is estimated to be ~1250 K (Yang, 1994). With similar calculations for the Fs_{25} orthopyroxene, the total estimated O3 displacement needed for the A chain to have the same configuration as the B chain is ~0.60 Å at 1200 K, whereas that for the B chain to have the same configuration as the A chain is ~0.99 Å. Therefore, it is more likely that the skew of the A chain will change from N to P at high temperature than the skew of the B chain in the Fs_{75} orthopyroxene. This explains why Fe-rich orthopyroxenes tend to transform to $C2/c$ clinopyroxenes instead of the protoenstatite structure at high temperatures, as observed experimentally (Smyth, 1969; Sueno and Kimata, 1981; Sueno and Prewitt, 1983; Sueno et al., 1985).

Fe-Mg order-disorder

The relationship between ln K_D (where $K_D = Fe^{M1}$-$Mg^{M2}/Fe^{M2}Mg^{M1}$) and $1/T$ (K) is linear from 1000 to 1200 K but shows an anomalous behavior between 1200 and 1300 K (see Fig. 2a of Yang and Ghose, 1994a). The observed anomalous temperature dependence of the Fe-Mg order-disorder may be attributed to the significant structural changes between 1200 and 1300 K. The pronounced straightening of the silicate B chain from 1200 to 1300 K causes the switching of the bridging O3B atoms within the M2 site coordination sphere. The resulting change in the electrical charge distribution primarily around the M2 site is probably responsible for the lowering of the disordering rate in this temperature range.

Acknowledgments

We thank D.H. Lindsley of SUNY at Stony Brook for help with the crystal synthesis, L.W. Finger of Geophysical Laboratory, Washington, DC, for providing the RFINE90 program, W.D. Scott of the University of Washington in Seattle for help in modifying the gas-flow furnace, M.J. Brown and M. Cai for providing the facilities for the evacuation and sealing of crystal mounts, and V. Schomaker for providing the THMA13 program. The critical comments and suggestions for improvement from C.T. Prewitt and an anonymous reviewer are greatly appreciated. The support of this research by the grants from NASA (NAG9-460 to J. Ganguly and S.G.), NSF (EAR-9117389 to S.G.), and the University of Washington Department of Geological Sciences Graduate Research Fund is gratefully acknowledged.

References cited

Anovitz, L.M., Essene, E.J., and Dunham, W.R. (1988) Order-disorder experiments on orthopyroxenes: Implications for the orthopyroxene geospeedometer. American Mineralogist, 73, 1060–1073.

Besancon, J.R. (1981) Rate of cation ordering in orthopyroxenes. American Mineralogist, 66, 965–973.

Boysen, H., Frey, F., Schrader, H., and Eckold, G. (1991) On the proto to ortho/clino enstatite phase transformation: Single crystal X-ray and inelastic neutron investigation. Physics and Chemistry of Minerals, 17, 629–635.

Brown, W.L., Morimoto, N., and Smith, J.V. (1961) A structural explanation of the polymorphism and transition of $MgSiO_3$. Journal of Geology, 69, 609–616.

Cameron, M., and Papike, J.J. (1981) Structural and chemical variations in pyroxenes. American Mineralogist, 66, 1–50.

Cameron, M., Sueno, S., Prewitt, C.T., and Papike, J.J. (1973) High-temperature crystal chemistry of acmite, diopside, hedenbergite, jadeite, spodumene and ureyite. American Mineralogist, 58, 594–618.

Coe, R.S. (1970) The thermodynamic effect of shear stress on the orthoclino inversion in enstatite and other coherent phase transitions characterized by a finite simple shear. Contributions to Mineralogy and Petrology, 26, 247–264.

Coe, R.S., and Kirby, S.H. (1975) The orthoenstatite to clinoenstatite transformation by shearing and reversion by annealing: Mechanism and potential applications. Contributions to Mineralogy and Petrology, 52, 29–55.

Ghose, S. (1965) Mg^{2+}-Fe^{2+} order in an orthopyroxene, $Mg_{0.93}Fe_{1.07}Si_2O_6$. Zeitschrift für Kristallographie, 122, 81–99.

Ghose, S., and Hafner, S. (1967) Mg^{2+}-Fe^{2+} distribution in metamorphic and volcanic orthopyroxenes. Zeitschrift für Kristallographie, 125, 1–6.

Ghose, S., Schomaker, V., and McMullan, R.K. (1986) Enstatite, $Mg_2Si_2O_6$: A neutron diffraction refinement of the crystal structure and a rigid-body analysis of the thermal vibration. Zeitschrift für Kristallographie, 176, 159–175.

Lee, W.E., and Heuer, A.H. (1987) On the polymorphism of enstatite. Journal of American Ceramic Society, 70, 349–360.

Murakami, T., Takeuchi, Y., and Yamanaka, T. (1982) The transition of orthoenstatite to protoenstatite and the structure at 1080°C. Zeitschrift für Kristallographie, 160, 299–312.

——— (1984) X-ray studies on protoenstatite: II. Effects of temperature on the structure up to near the incongruent melting point. Zeitschrift für Kristallographie, 166, 263–275.

——— (1985) High-temperature crystallography of a protopyroxene. Zeitschrift für Kristallographie, 173, 87–96.

Ohashi, Y., and Finger, L.W. (1973) A possible high-low transition in orthopyroxene and orthoamphiboles. Carnegie Institution of Washington Year Book, 72, 544–547.

Pannhorst, W. (1979) Structural relationships between pyroxenes. Neues Jahrbuch für Mineralogie Abhandlungen, 135, 1–17.

——— (1982) Interpretation of the diffuse X-ray reflections observed in orthoenstatite inverted from low-clinoenstatite. Neues Jahrbuch für Mineralogie Abhandlungen, 145, 270–279.

Robinson, K., Gibbs, G.V., and Ribbe, P.H. (1971) Quadratic elongation: A quantitative measure of distortion in coordination polyhedra. Science, 172, 567–570.

Sadanaga, R., Okmura, F.P., and Takeda, H. (1969) X-ray study of the phase transition of enstatite. Mineralogical Journal, 6, 110–130.

Saxena, S.K., and Ghose, S. (1971) Mg^{2+}-Fe^{2+} order-disorder and the thermodynamics of the orthopyroxene crystalline solution. American Mineralogist, 56, 532–559.

Saxena, S.K., Domeneghetti, M.C., Molin, G.M., and Tazzoli, V. (1989) X-ray diffraction study of Fe^{2+}-Mg order-disorder in orthopyroxene: Some kinetic results. Physics and Chemistry of Minerals, 16, 421–427.

Schomaker, V., and Trueblood, K.N. (1968) On the rigid-body motion of molecules in crystals. Acta Crystallographica, B24, 63–74.

Schrader, H., Boysen, H., Frey, F., Convert, P. (1990) On the phase transformation proto- to clino-/orthoenstatite: Neutron powder investigation. Physics and Chemistry of Minerals, 17, 409–415.

Smith, J.V. (1969) Crystal structure and stability of the $MgSiO_3$ polymorphs: Physical properties and phase relations of Mg-Fe pyroxenes. Mineralogical Society of America Special Papers, 2, 3–30.

Smyth, J.R. (1969) Orthopyroxene-high-low clinopyroxene inversions. Earth and Planetary Science Letters, 6, 406–407.

Smyth, J.R. (1973) An orthopyroxene structure up to 850°C. American Mineralogist, 58, 636–648.

Smyth, J.R. (1974) Experimental study on the polymorphism of enstatite. American Mineralogist, 59, 345–352.

Smyth, J.R., and Burnham, C.W. (1972) The crystal structure of high and low clinohypersthene. Earth and Planetary Science Letters, 14, 183–189.

Sueno, S., and Kimata, M. (1981) On the ortho-clino phase transition of ferrosilite ($FeSiO_3$) and Fe-rich pyroxenes. Acta Crystallographica, A37, C-111.

Sueno, S., and Prewitt, C.T. (1983) Models for the phase transition between orthoferrosilite and high clinoferrosilite. Fortschritte der Mineralogie, 61, 223–241.

Sueno, S., Cameron, M., and Prewitt, C.T. (1976) Orthoferrosilite: High temperature crystal chemistry. American Mineralogist, 61, 38–53.

Sueno, S., Kimata, M., and Prewitt, C.T. (1984) The crystal structure of high clinoferrosilite. American Mineralogist, 69, 264–269.

Sueno, S., Prewitt, C.T., and Kimata, M. (1985) Structural aspects of phase transitions in Fe-Mg-Ca pyroxenes. American Mineralogist, 70, 141–148.

Sykes-Nord, J.A., and Molin, G.M. (1993) Mg-Fe order-disorder in Fe-rich orthopyroxenes: Structural variations and kinetics. American Mineralogist, 78, 921–931.

Trueblood, K.N. (1978) Analysis of molecular motion with allowance for intermolecular torsion. Acta Crystallographica, A34, 950–954.

Turnock, A.C., Lindsley, D.H., and Grover, J.E. (1973) Synthesis and unit cell parameters of Ca-Mg-Fe pyroxenes. American Mineralogist, 58, 50–59.

Virgo, D., and Hafner, S.S. (1969) Order-disorder in heated orthopyroxenes. Mineralogical Society of America Special Paper, 2, 67–81.

Yang, H. (1994) High temperature single-crystal X-ray diffraction studies of synthetic $(Fe,Mg)_2Si_2O_6$ orthopyroxenes: Thermal expansion, crystal structure and thermodynamic properties. Ph.D. thesis, University of Washington, Seattle, Washington.

Yang, H., and Ghose, S. (1994a) In-situ Fe-Mg order-disorder studies and thermodynamic properties of orthopyroxene $(Mg,Fe)_2Si_2O_6$. American Mineralogist, 79, 633–643.

——— (1994b) Thermal expansion, Debye temperature and Grüneisen parameter of synthetic $(Fe,Mg)SiO_3$ orthopyroxenes. Physics and Chemistry of Minerals, 20, 575–586.

Manuscript received January 28, 1994
Manuscript accepted September 19, 1994